

The use of pulse synthesis for optimization of photoacoustic measurements

Adi Sheinfeld^{*†}, Elad Bergman[†], Sharon Gilead and Avishay Eyal

School of Electrical Engineering, Faculty of Engineering, Tel-Aviv University, Ramat Aviv, Tel-Aviv, 69978, Israel

^{*}Corresponding author: adishein@post.tau.ac.il

[†] These authors contributed equally to this work

Abstract: In this paper the use of pulse shaping in photoacoustic (PA) measurements is presented. The benefits of this approach are demonstrated by utilizing it for optimization of either the responsivity or the sensitivity of PA measurements. The optimization is based on the observation that the temporal properties of the PA effect can be represented as a linear system which can be fully characterized by its impulse response. Accordingly, the response of the PA system to an input optical pulse, whose instantaneous power is arbitrarily shaped, can be analytically predicted via a convolution between the pulse envelope and the PA impulse response. Additionally, the same formalism can be used to show that the response of the PA system to a pulse whose instantaneous power is a reversed version of the impulse response, i.e. a matched pulse, would exhibit optimal peak amplitude when compared with all other pulses with the same energy. Pulses can also be designed to optimize the sensitivity of the measurement to a variation in a specific system parameter. The use of the matched pulses can improve SNR and enable a reduction in the total optical energy required for obtaining a detectable signal. This may be important for applications where the optical power is restricted or for dynamical measurements where long integration times are prohibited. To implement this new approach, a novel PA optical setup which enabled synthesis of excitation waveforms with arbitrary temporal envelopes was constructed. The setup was based on a tunable laser source, operating in the near-IR range, and an external electro-optic modulator. Using this setup, our approach for system characterization and response prediction was tested and the superiority of the matched pulses over other common types of pulses of equal energy was demonstrated.

©2009 Optical Society of America

OCIS codes: (300.6430) Spectroscopy: photothermal; (300.1030) Spectroscopy: Absorption; (170.5120) Medical Optics and Biotechnology: Photoacoustic Imaging

References and links

1. J.G. Laufer, C. Elwell, D. Delpy, and P. Beard, "In vitro measurements of absolute blood oxygen saturation using pulsed near-infrared photoacoustic spectroscopy: Accuracy and resolution," *Phys. Med. Biol.* **50**, 4409-4428 (2005).
2. X. Wang, Y. Pang, G. Ku, X. Xie, G. Stoica, and L.V. Wang, "Noninvasive laser-induced photoacoustic tomography for structural and functional in vivo imaging of the brain," *Nat. Biotechnol.* **21**, 803-806 (2003).
3. A. C. Tam, "Applications of PA sensing techniques," *Rev. Mod. Phys.* **58**, 381-431 (1986).
4. H. M. Lai and K. Young, "Theory of the pulsed photoacoustic technique," *J. Acoust. Soc. Am.* **72**, 2000-2007 (1982).
5. G. J. Diebold, T. Sun, and M. I. Khan, "Photoacoustic monopole radiation in one, two and three dimensions," *Phys. Rev. Lett.* **67**, 3384-3387 (1991).
6. R. A. Kruger, P. Liu, Y. R. Fang, and C. R. Appledorn, "Photoacoustic ultrasound – reconstruction tomography," *Med. Phys.* **22**, 1605-1609 (1995).
7. E. Bergman, A. Sheinfeld, S. Gilead, and A. Eyal, "The use of optical waveform synthesis in photoacoustic measurements" in *Proceedings of IEEE 25th convention in Israel*, 585-588 (2008).
8. K. M. Quan, G. B. Christison, H. A. MacKenzie, and P. Hodgson, "Glucose determination by a pulsed photoacoustic technique: an experimental study using a gelatin-based tissue phantom," *Phys. Med. Biol.* **38**, 1911-1922 (1993).

9. A. J. Sadler, J. G. Horsch, E. Q. Lawson, D. Harmatz, D. T. Brandau, C. R. Middaugh, "Near-infrared photoacoustic spectroscopy of proteins," *Anal. Biochem.* **138**, 44-51 (1984).
 10. Y. Wang, D. Xing, Y. G. Zeng, and Q. Chen, "Photoacoustic imaging with deconvolution algorithm," *Phys. Med.* **49**, 3117-3124 (2004).
 11. J. G. Proakis, *Digital Communications, 4th Edition* (McGraw-Hill, 2001), Chap. 5.
-

1. Introduction

Photoacoustic (PA) measurements have found many applications in various fields, such as spectroscopy [1], imaging and tomography [2] and more. The photoacoustic technique is based on measuring the acoustic signal generated due to the absorption of modulated light in the tested medium and the associated thermal expansion [3].

The theory behind the photoacoustic effect is well known for decades and the underlying equation has been studied by many authors ([4,5,6] for example). Under rather general conditions it is a linear wave equation with a source function which depends on the intensity of the optical excitation and on some physical parameters of the medium. Exploiting its linearity, it is possible to express the solution to the photoacoustic equation as a convolution of the input temporal pulse with the system impulse response [6]. This characteristic of the photoacoustic effect opens the possibility to use methods of linear systems design and analysis to optimize different aspects of the measurement technique. In particular, in this work we studied two examples which demonstrate the use of pulse pre-shaping for PA optimization: in the first example the responsivity of the PA setup was optimized by using an excitation pulse that was designed to maximize the acoustic peak response, for a given pulse energy. In the second example, the envelope of the excitation pulse was tailored to optimize the sensitivity of the PA measurement to a variation in the concentration of one substance in a liquid mixture. As shown in sec. 2, this approach is rather general and it is possible to design pulses which optimize the sensitivity of the PA measurement to many other parameters. The use of such optimal pulses enables a reduction in the total optical energy required for obtaining a detectable signal and may be important in applications where the optical power is restricted or in dynamical measurements where short integration time is needed.

Until now, pulsed photoacoustic measurement techniques have been relying predominantly on pulsed laser sources. Among these sources the Q-switched Nd:YAG laser is probably the most popular. While such sources are a very practical choice for photoacoustic measurements due to their robustness, high-power and cost, they possess one major drawback: they offer a rather limited control over the temporal shape and properties of the generated pulses. Recently we introduced a novel optical setup that allows synthesis of excitation pulses with arbitrary temporal shapes for PA measurements [7]. The setup is based on a CW tunable laser source modulated by an electro-optic modulator which is driven by an arbitrary waveform generator (AWG). An Erbium Doped Fiber Amplifier (EDFA) is used to amplify the modulated excitation signal.

The particular setup that was constructed takes advantage of the mature technology and components which are available for fiber-optic communications. It is operating in the fiber-optic C band (around 1550nm) which belongs to the near-IR (NIR) spectral range. PA measurements in this spectral range were studied by several authors for various applications, such as glucose monitoring [8] and proteins characterization [9]. Clearly pulse pre-shaping can be used also at other spectral ranges by implementing suitable modulation techniques.

To use the proposed setup for optimization of the excitation pulse, the following two-stage procedure was developed; first, the impulse response of the PA measurement setup, or its derivative with respect to a monitored parameter, was found. The linearity of the system ensures that once the impulse response is obtained, the acoustical response to any other input optical pulse can be predicted. In particular, it is possible to show that by shaping the optical excitation pulse as the time-reversed impulse response, the resulting acoustic output exhibits a maximum peak magnitude which is higher than the peak magnitudes that correspond to all other pulses of different shape and equal energy. Alternatively, if the excitation pulse is taken to be a time-reversed version of the derivative of the impulse-response with respect to a

chosen parameter, the sensitivity of the PA measurement to local variations in this parameter is optimized. In PA systems where the noise and the signal are uncorrelated, as was empirically verified for the setup used in this study, the maximum responsivity pulse is also optimal in terms of Signal to Noise Ratio (SNR). In the second stage, the instantaneous intensity of the optical pulse was shaped in the form of the optimal pulse by feeding the tailored pulses to the AWG and the resulting response was recorded.

The paper is organized as follows: in sec. 2 the theory of PA response prediction and optimization is described. The experimental setup which enables pulse synthesis and the experimental verification of the theory are described in sec. 3 and sec. 4 respectively. Sec. 5 discusses the more system-specific issues of noise and stability and sec. 6 comprises a summary and discussion of further potential applications.

2. Theory

The Photoacoustic (PA) effect refers to the generation of acoustical waves due to the irradiation of an absorbing medium by modulated light. The temperature rise which follows the absorption leads to thermal expansion which, in turn, leads to pressure variations that propagate in the medium as an acoustical wave. When the optical power is sufficiently low, the most dominant process that generates photoacoustic pressure waves is the thermoelastic effect, and other processes, such as electrostriction for example, can be neglected. If the duration of the light pulse is shorter than the thermal relaxation time, the heat generated by its absorption remains confined in the irradiated volume during the laser pulse. This situation is commonly described as “thermal confinement”. Under this condition, the generation and propagation of the pressure wave, $p(\mathbf{r}, t)$, in a liquid medium, can be described by the following wave equation [4]:

$$\frac{1}{c^2} \frac{\partial^2 p(\mathbf{r}, t)}{\partial t^2} - \nabla^2 p(\mathbf{r}, t) = \frac{\alpha\beta}{C_p} \frac{\partial I(\mathbf{r}, t)}{\partial t} \quad (1)$$

where c is the sound velocity, β is the volumetric thermal expansion coefficient, C_p is the specific heat, α is the absorption coefficient and $I(\mathbf{r}, t)$ is the intensity of the impinging light.

Due to the enormous difference between the optical and acoustical speeds, it can be assumed that the temporal variations in the light intensity propagate almost instantaneously to the entire medium. According to this assumption, the spatial and temporal dependences of the optical intensity become decoupled and the intensity can be expressed as: $I(\mathbf{r}, t) = g(\mathbf{r}) \cdot f(t)$, where $g(\mathbf{r})$ describes the spatial distribution of the intensity and $f(t)$ describes the temporal modulation. Using the separated form of the intensity and the linearity of the PA equation, it is possible to express the solution to Eq. (1) as:

$$p(\mathbf{r}, t) = H(\mathbf{r}, t) * f(t) = \int_{-\infty}^{\infty} H(\mathbf{r}, t - \tau) f(\tau) d\tau \quad (2)$$

where $H(\mathbf{r}, t)$, the PA impulse response, satisfies:

$$\frac{1}{c^2} \frac{\partial^2 H(\mathbf{r}, t)}{\partial t^2} - \nabla^2 H(\mathbf{r}, t) = \frac{\alpha\beta}{C_p} g(\mathbf{r}) \frac{d}{dt} [\delta(t)] \quad (3)$$

Equations (2)-(3) show that the PA measurement can be represented as a linear system whose impulse response, $H(\mathbf{r}, t)$, is completely determined by the medium parameters, the spatial distribution of the optical intensity and the boundary conditions. Furthermore, once $H(\mathbf{r}, t)$ is measured at a given point in space, \mathbf{r}_{meas} , it is possible to analytically predict the response of the PA measurement system, at this position, to any other optical excitation pulse

via the convolution in Eq. (2). In case of a homogeneous medium it is possible to use a Green function to solve the wave equation, in which case the impulse response can be calculated analytically, as was shown by Kruger *et al* [6] and Wang *et al* [10].

Formulating the PA measurement as a linear system, and our ability to synthesize excitation pulses with general waveforms, can also be useful for optimization of the responsivity of the system. Assuming $H(\mathbf{r}_{\text{meas}}, t)$ is zero outside the time interval $0 \leq t \leq T$, it is well known from the theory of linear systems (Proakis for example [11]) that a pulse with a matched envelope, $f(t) = aH(\mathbf{r}_{\text{meas}}, T - t)$, where a is a normalization factor, produces a peak response at $t = T$ which is higher than the response of any other input pulse with the same energy $\varepsilon = \int_0^T |f(t)|^2 dt$. Under the condition that the noise and the signal are uncorrelated, this pulse also yields the optimal SNR among all pulses with the same optical energy. As was verified experimentally in the system that we studied (sec. 5), the noise level was independent of the signal amplitude and hence the above condition was satisfied.

Another example which highlights the usefulness of pulse pre-shaping is optimization of the sensitivity of the PA measurement to a variation in a pre-specified system-parameter. The specific system-parameter that is selected depends on the application: it may be a concentration of a substance in a mixture or a solution, the optical wavelength of the tunable laser in spectral measurements of absorption coefficient, or any other parameter which affects the PA response and can be controlled. Denoting this parameter by ρ , it is readily obtained from Eq. (2) that:

$$\frac{\partial p(\mathbf{r}, t, \rho)}{\partial \rho} = \frac{\partial H(\mathbf{r}, t, \rho)}{\partial \rho} * f(t) \quad (4)$$

Clearly, an input pulse whose envelope is of the form: $f(t) = a \partial H(\mathbf{r}_{\text{meas}}, T - t, \rho) / \partial \rho$ maximizes $\partial p(\mathbf{r}_{\text{meas}}, t, \rho) / \partial \rho$ and ensures optimal sensitivity to variations in ρ . The use of this approach for optimizing the sensitivity of a PA setup for variations of the concentration of water inside an Ethanol-water mixture, is experimentally demonstrated in sec. 3-4.

The use of a matched pulse requires a preliminary measurement of the systems impulse response. It is clear that any change in the setup that occurs after the preliminary measurement may induce a variation in $H(\mathbf{r}_{\text{meas}}, t)$ that will affect the magnitude of the response. As shown in sec. 5, in our experimental setup the effect of environmental instabilities on $H(\mathbf{r}_{\text{meas}}, t)$ was more pronounced towards its trailing edge than near its leading edge. In light of this observation we studied the effect of using a truncated matched pulse which is defined by:

$$f_{\text{trun}}(t, \tilde{T}) = \begin{cases} aH(\mathbf{r}_{\text{meas}}, \tilde{T} - t) & 0 \leq t \leq \tilde{T} < T \\ 0 & \text{elsewhere} \end{cases} \quad (5)$$

The corresponding peak response is obtained by substituting $f_{\text{trun}}(t, \tilde{T})$ in Eq. (2) and then setting $t = \tilde{T}$:

$$p_{\text{trun}}(\mathbf{r}_{\text{meas}}, \tilde{T}) = a \int_0^{\tilde{T}} |H(\mathbf{r}_{\text{meas}}, \tau)|^2 d\tau \quad (6)$$

The ratio between the response of a truncated matched pulse and the response of a full-length matched pulse with the same energy can be found by using Eq. (6) and the proper normalization factors:

$$\frac{p_{\text{trun}}(\mathbf{r}_{\text{meas}}, \tilde{T})}{p(\mathbf{r}_{\text{meas}}, T)} = \frac{\sqrt{\int_0^{\tilde{T}} |H(\mathbf{r}_{\text{meas}}, \tau)|^2 d\tau}}{\sqrt{\int_0^T |H(\mathbf{r}_{\text{meas}}, \tau)|^2 d\tau}} \quad (7)$$

As expected, according to this relation the PA response can only be improved by increasing \tilde{T} and the maximum response is obtained when $\tilde{T}_{\text{optimal}} = T$. It is shown in sec. 5, however, that measurement instabilities may moderate this improvement and in some cases they can even lead to a decrease in the response for pulses longer than some $\tilde{T}_{\text{optimal}} < T$.

3. The experimental setup and the measurement method

The experimental setup is shown in Fig. (1).

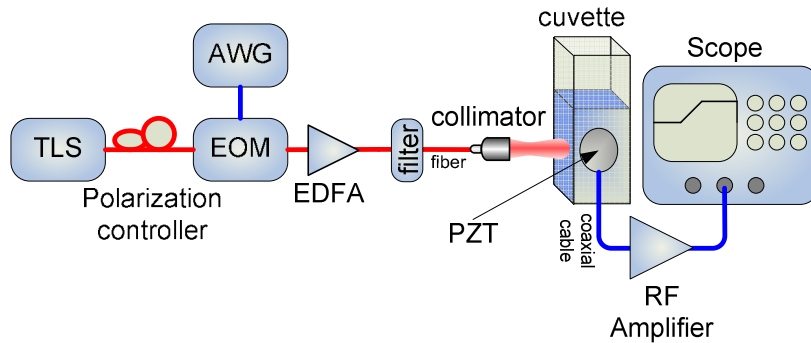


Fig. 1. A PA experimental setup enabling the use of pulses with arbitrary envelopes

The optical part comprised a fiber-coupled Tunable Laser Source (TLS) in the range of 1510-1620nm, a polarization controller, a Lithium-Niobate Electro-Optic Modulator (EOM) driven by an Arbitrary Waveform Generator (AWG) and an Optical Erbium Doped Fiber Amplifier (EDFA) followed by an optical filter. The use of the modulator and the AWG enabled synthesis of pulses with arbitrary temporal shapes. The output of the optical filter was collimated and the beam was directed into a cell containing the tested liquid. The acoustical detection circuit used a ceramic piezoelectric transducer (PZT), with resonance frequency at 200KHz and a fractional bandwidth of 70% (measured when it was glued to the cell). The PZT output was amplified by an RF amplifier (with a cutoff frequency at 1MHz) whose output was sampled and averaged over at least 500 pulses by a digital oscilloscope. The relatively narrow bandwidths of the RF amplifier and PZT that were available for us for this work limited the temporal resolution to the microseconds range. This limitation, however, is not fundamental and can be easily overcome by using an amplifier and PZT with a broader band.

The tested liquid chosen for this study was ethanol, due to its high optical-power to acoustical-power conversion efficiency. This characteristic of ethanol is a result of its significant absorption near 1550nm and its low specific heat and high thermal expansion coefficient. In the second experiment for sensitivity enhancement we used mixtures of ethanol and water, which differ in their absorption and thermal coefficients and in their acoustic velocities.

As described in sec. 2, the first step in characterizing the system and in finding the optimal pulse is a measurement of the impulse response. To approximate the impulse at the system input it was required to generate an optical pulse whose duration is as short as possible and its

peak power is as high as possible. In the external modulation scheme that was used, pulse durations as short as few nanoseconds could be easily generated, however the maximum peak power was limited to 100mW, leading to pulse optical energy in the range of 1 μ Joule. Due to this limitation, the best approximated impulse at the input yielded a very weak acoustical response. In order to overcome this difficulty we measured the step-response of the system rather than the impulse response (a step input was approximated by long square pulses of ~ 1.5 ms) and obtained the impulse response by numerically differentiating the step response.

To demonstrate the viability of our technique in both experiments, we compared between the response of the PA system to the matched pulse and its responses to optimal square and Gaussian input pulses. Since the pulse energy varied according to its shape, all responses were normalized by the optical-pulse energy that was measured simultaneously with the PA measurement. The optimal durations of the square and Gaussian pulses were numerically predicted using the measured impulse response and Eq. (2) and this prediction was experimentally verified.

4. Experimental results – PA impulse response and pulse pre-shaping

An example of the measured step response of the PA system, as well as the input step signal are shown in Fig. (2). The corresponding matched pulse, $f_{\text{trun}}(t, \tilde{T})$, truncated to $\tilde{T} = 40\mu\text{sec}$, was produced from the derivative of the step response in accord with Eq. (4) (Fig. (3)).

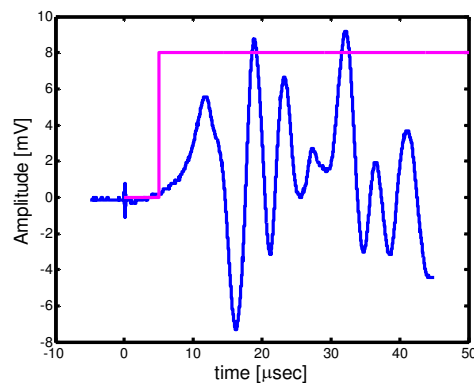


Fig. 2. A step input (pink) and the corresponding PA step response (blue).

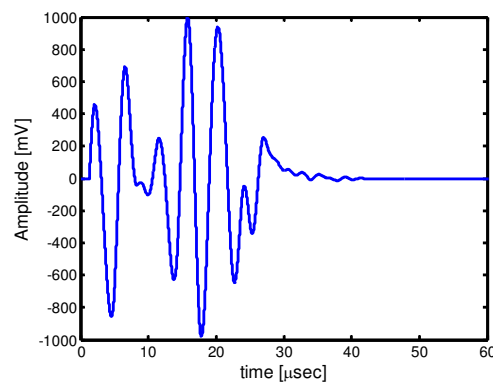


Fig. 3. A truncated time-reversed impulse response. This waveform was fed to the AWG to produce an enhanced PA response.

Once the impulse response was known, it was possible to use it for predicting the response of the system to an arbitrary input. Examples of measured and predicted responses to the matched pulse and to a Gaussian pulse are shown in Figs. (4) and (5) respectively. The good agreement between the measurement and the prediction is clearly seen. The deviation in Fig. (4) of the predicted response from the measured response for $t > 25\mu\text{sec}$ is due to the truncation of the impulse response.

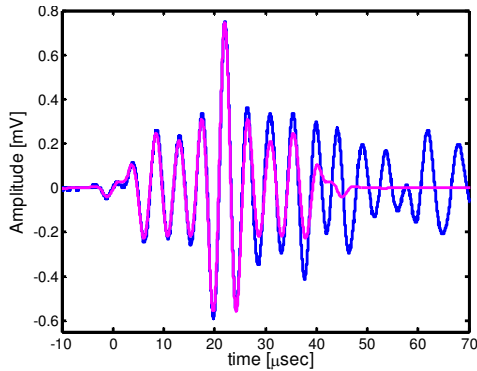


Fig. 4. The measured (blue) and predicted (pink) PA response to a matched pulse.

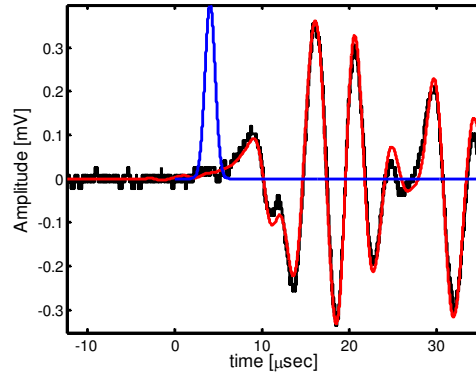


Fig. 5. The measured (black) and predicted (red) PA response to a Gaussian input (blue) with FWHM width of $1.4\mu\text{sec}$.

In the first experiment, which tests responsivity optimization, we compared the matched-pulse response to the responses to pulses with either a Gaussian or square envelopes. We chose these two examples since these envelopes appear frequently in studies of pulsed PA measurements. In order to demonstrate the enhanced peak response of the matched pulse we first utilized Eq. (2) to numerically find the optimal widths of the Gaussian and square pulses. Plots of the dependence of the peak response of the Gaussian and square pulses as a function of their widths are shown in Fig. (6), in addition to experimental data that verifies the numerical calculation. It can be seen from these plots that the optimal square pulse width is $1.29\mu\text{sec}$ and optimal Gaussian pulse FWHM is $1.13\mu\text{sec}$. Figure (7) shows the measured PA responses to the matched pulse and to the optimal Gaussian and square pulses. The advantage of using a matched pulse, which yielded a factor of two improvement in the peak amplitude compared with the other pulses, is clearly seen. Note the similarity between the responses to the optimal square and Gaussian pulses. This is attributed to the limited bandwidth of the system which caused a filtering of the high frequency components of the response to the square pulse.

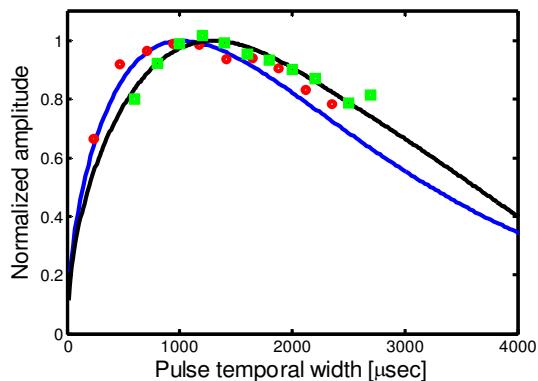


Fig. 6. The peak response of Gaussian (analytical calculation – blue line, experimental data – red circles) and square (numerical calculation – black line, experimental data – green squares) pulses as a function of their widths (the width of the Gaussian pulse is defined to be its FWHM):

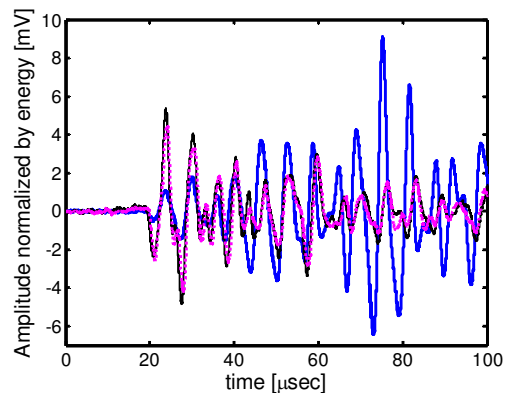


Fig. 7. The measured PA response of the matched pulse (blue), the optimal Gaussian pulse with FWHM= $1.13\mu\text{sec}$ (black) and the optimal square pulse with time duration = $1.29\mu\text{sec}$ (dotted pink).

As described in sec. 2, matched pulses can be used for optimization of the systems sensitivity as well as its responsivity. In the second experiment this unique application of our setup is demonstrated by optimizing the sensitivity of the PA measurement to small variations in the concentration of water in Ethanol-water mixtures. These variations change the absorption coefficient, the thermal coefficients and the acoustic velocity of the mixture and in turn its PA response.

A pulse which approximates the theoretically predicted optimal pulse was constructed by measuring the impulse responses for two concentrations of water (10% and 20%), inverting them in time and finding their difference, which approximates the local derivative:

$\partial_c H(\mathbf{r}, T - t, C) \approx H(\mathbf{r}, T - t, 10\%) - H(\mathbf{r}, T - t, 20\%) = f_{10-20}(t)$ (C denotes concentration). In addition, we used the measured impulse responses to predict the responses to Gaussian and square pulses and to numerically find the parameters of the Gaussian and square pulses that maximize the sensitivity to local variations in water concentration. This was done in the same method described for the first experiment, however here the convolution was done with the impulse derivative approximation $f_{10-20}(t)$ rather than the impulse response. The FWHM of the optimal Gaussian pulse was found to be $1.036\mu\text{s}$ and the optimal square pulse was $1.3\mu\text{s}$ long. The three pulses – the approximated impulse response derivative, the optimal Gaussian pulse and square pulse were fed to the AWG. As was described in sec. 2, when the optimal pulse is used it ensures maximum sensitivity of the response to variation in the perturbed parameter at a specific point in time which was denoted by T . Figure (8) shows the normalized PA responses at $t = T$, for the approximated optimal pulse, $f_{10-20}(t)$, versus water concentration in the range where the derivative was obtained. Also shown are the normalized responses of the optimal Gaussian and square pulses at their optimal times T_{max_G} and T_{max_S} respectively. The superiority of the matched pulse is clearly seen. Note that the ability to produce the optimal Gaussian and square pulses is also a feature of our setup and that non-optimized Gaussian and square pulses will perform even worse.

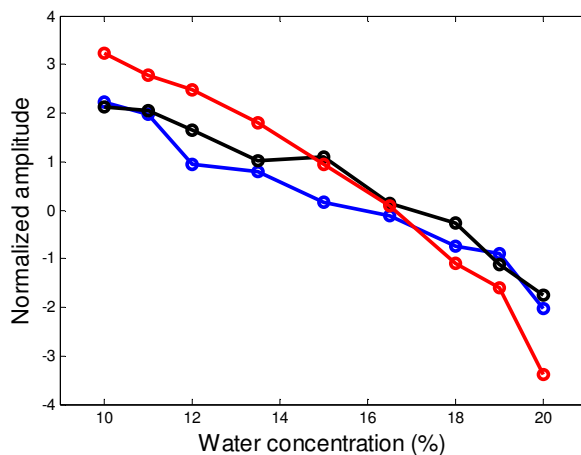


Fig. 8. Normalized PA responses versus water concentration in Ethanol-Water mixture: matched pulse at $t=T$ (red), optimal Gaussian pulse at $t=T_{\text{max}_G}$ (blue), optimal square pulse at $t=T_{\text{max}_S}$ (black).

5. Experimental results - noise and stability

As discussed in sec. 2, in the presence of noise the use of the matched pulse, which yields the maximum peak response, would also ensure optimal SNR, provided that the noise is independent of the signal amplitude. To study the noise characteristics of our setup, the PA responses of several types of input pulses were repeatedly measured for 50 times. For each type of response, the mean values of all local extrema and the corresponding standard deviations (STDs) were calculated. A scatter diagram of the STD values versus the mean amplitudes is presented in Fig. (9). Both values were normalized by the maximum peak amplitude. It can be observed that the normalized STD values, characterizing the system noise, are scattered around 0.02 and does not show any correlation with the signal amplitude. A quantitative measure to this observation is the correlation coefficient between the two vectors of data which was found to be -0.05.

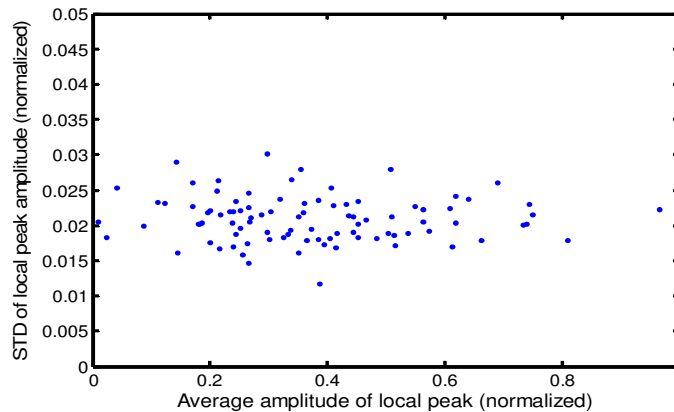


Fig. 9. Standard deviation of the local extrema of the PA response vs. their mean amplitudes. Both values were calculated over 50 samples and normalized by the maximum peak value. The corresponding correlation coefficient was found to be -0.05.

In addition to noise, a typical PA measurement setup is affected by environmental instabilities. As described in sec. 2, the PA impulse response is a solution to Eq. (3) given the medium parameters and the optical-source spatial-distribution, $g(\mathbf{r})$, and subject to the specific boundary conditions of the PA system. In realistic experimental situations, however, the PA system may be affected by environmental instabilities such as temperature variations, mechanical vibrations etc. which can lead to variations in its impulse response. These variations in the impulse response can cause a deviation of the predicted PA response from the measured response or suboptimal response to the “matched” pulse. The effect of environmental instabilities is demonstrated in Fig. (10). It shows 3 consecutive PA step responses that were recorded with intermissions of approximately 5 minutes. It can be seen that the effect of instabilities is more pronounced towards the trailing edge of the response than near the leading edge. In light of this observation, the use of truncated matched pulses was studied. According to Eq. (7), in ideal conditions the peak PA response is a monotonically increasing function of the truncation time \tilde{T} , but due to instabilities, in realistic conditions this may no longer be true. This can be observed in Fig. (11), where calculated normalized peak responses are plotted as a function of the truncation time. These numerical estimations of matched-pulse responses were calculated from measured impulse responses with the use of Eq. (2). The blue plot represents a perfectly stable system. It was calculated by convolving an impulse response with its truncated and reversed versions. In all other plots the convolution is between the truncated matched pulse and an impulse response which was recorded between 5 to 30 minutes after the first impulse response which was used

for the matched pulse synthesis. It can be seen that due to the instability of the impulse response the peak response is not optimal. Moreover, in some cases there exists a truncation time, $\tilde{T}_{optimal} < T$, for which the peak response reaches a maximum and an additional increase in the truncation time leads to a decrease in the response rather than an increase. The analysis leading to Fig. (11) can be used in order to determine the optimal truncation time in a given PA setup.

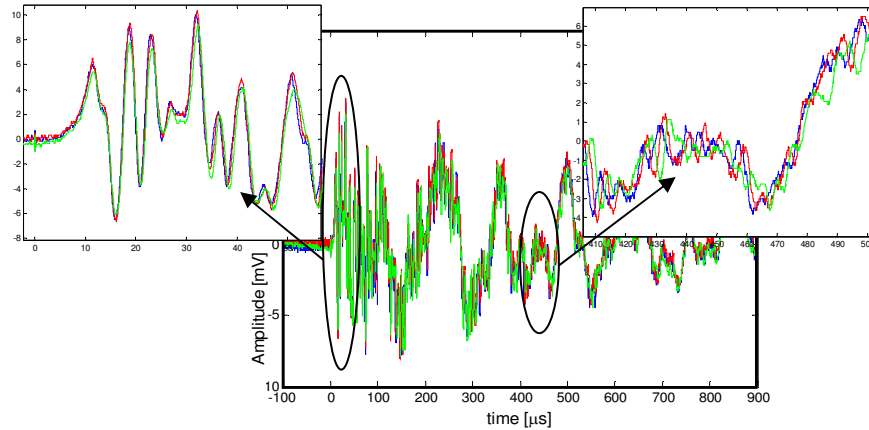


Fig. 10. Three examples of the PA step response taken with intermissions of 5 minutes between them. The insets demonstrate the increased mismatch between the responses at times approaching the trailing edge of the response.

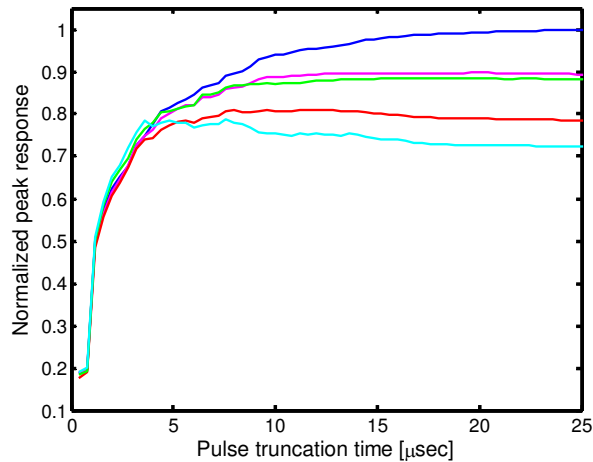


Fig. 11. Calculation of the peak PA response to truncated pulses as a function of truncation time. The blue plot represents a stable system where there is a perfect match between the truncated pulse and the impulse response. All other plots (pink, green, red and cyan) are examples of responses of the system to a non-perfectly matched pulse.

6. Conclusions

In this work a novel method for enhancement of the responsivity as well as the sensitivity of PA measurements was studied both theoretically and experimentally. The method is based on the linearity of the PA effect. It is shown that a PA measurement setup can be represented as a linear system with the time-dependent intensity of the optical excitation as its input and the amplified response of the acoustical transducer as its output. Using this formalism it is possible to characterize the system via its impulse response or equivalently via its step response. Once either of these responses is measured it is possible to predict the response of the PA setup to any other input. In particular, it is easy to show that the response of the system to a time-reversed version of the measured impulse response, i.e. to a matched pulse, will exhibit optimal peak amplitude. Alternatively, a pulse matching the derivative of the impulse response with respect to a targeted parameter can optimize the sensitivity of the setup to small variations in this parameter. Clearly, in situations where the impulse response changes significantly from one PA measurement to the other, these methods may not be practical, due to the need to re-measure the impulse response. However, in many cases the PA system is relatively stationary and the PA measurement is intended to detect small variations around a fixed operation point.

In order to implement this approach, an optical setup which enables synthesis of the envelope of the PA excitation pulse was required. Such a setup was constructed by using a tunable laser source in the NIR range and an external electro-optic modulator. Using this setup, our approach for system characterization and response prediction was tested and the superiority of the matched pulses over other common types of pulses of equal energy was demonstrated.

The use of a matched pulse with an optimal response may be important in cases where low optical excitation power is critical and in dynamical measurements where long integration times are prohibited. Our setup allows the flexibility to tailor an optimal pulse to a specific PA measurement application, which will be optimally sensitive to variations in the tested parameter.

The effect of system instabilities on the matched pulse measurement approach was also studied. It was shown that the measured peak amplitude was affected by instabilities and a judicious choice of the truncation time of the impulse response was useful in limiting this effect.

Finally, we wish to note that the unique optical configuration of the setup, which enables flexibility in controlling the excitation waveform, may be used in a variety of other applications, which cannot be implemented in most common PA setups, such as: enhancement of spatial resolution through pulse compression or coding or by superimposing the pulse on an RF carrier. Such applications are currently under study.

Acknowledgment

This work was supported by the Israeli Science Foundation (ISF).